# Impact of polyelectrolytes on lysozyme properties in colloidal dispersions

Mbaye Ndour, Jean-Marc Janot, Laurence Soussan, Zaineb Bouaziz, Damien Voiry, Sebastien Balme

# Impact of Polyelectrolytes on Lysozyme Properties in Colloidal Dispersions.

Ndaye Ndour, Jean-Marc Janot, Laurence Soussan, Zaineb Bouaziz, Damien Voiry, Sebastien Balme*

*Institut Européen des Membranes, IEM – UMR 5635, ENSCM, CNRS, Univ Montpellier, Montpellier, France*

Corresponding author: sebastien.balme@umontpellier.fr

**Statistical summary: 5198 words; 3 figures, 3 tables**

**Abstract**

In this work, we investigated the impact of different polyelectrolytes (polyacrylic acid, polystyrene sulfonate, dextran sulfate, and chondroitin sulfate) on lysozyme properties when they form colloidal complexes. To this aim, we characterized (i) the size and stability of the different polyelectrolyte-lysozyme complexes upon addition of NaCl (different concentrations) by diffusion light scattering, and (ii) the structure and accessibility of lysozyme active site in such complexes by fluorescence quenching and time resolved fluorescence analysis. We then used these results to explain the antibacterial activity variations among colloidal complexes and compared with free lysozyme. Our findings show that colloidal complexes that are more prone to swelling (i.e., lysozyme complexed with polystyrene sulfonate) are less stable upon salt addition. In these colloids, the enzymatic site is also more accessible. However, the antibacterial activity does not depend on the swelling properties because no large structural modification of the active site occurs.

## 1. Introduction

Polyelectrolyte (PE)-protein complexes have been widely studied due to their numerous applications, such as protein delivery, catalysis, biosensing, and protein separation[1]. These complexes adopt different structures (colloidal suspension, gel, and turbid solution[2]) depending on the balance of negative/positive charges. This balance is usually governed by the ratio of protein/PE concentrations and pH[3]. In water media, PE/protein complexes are typically governed by electrostatic interactions, and often become instable at high ionic strength when the salts shield the PE charges[2,4]. In several cases, hydrogen (H-) bonds can compete with electrostatic interactions[1]. Regardless of the nature of the application, a key point of these complexes is the structural modification of the complexed proteins. More specifically for catalysis or biosensing as well as for drug delivery and entrapment, the enzyme active site must be preserved and must remain accessible[5,6] [7,8].

Lysozyme is a model of hard protein with a well-known structure[9,10]. It is composed of 129 amino acid residues divided in two main domains: the α-domain made of α-helices, and the β-domain that consists mainly of β-sheets. Between these domains a loop completes the enzymatic site that catalyzes the hydrolysis of the glycosidic β (1-4) linkages between N-acetylglucosamine and N-acetylmuramic acid into peptidoglycans, contributing to lysozyme antibacterial property. From an energetic point of view, lysozyme exhibits a high internal energy of about 60 kJ $mol^{-1}$ due to the large ratio of β-sheets and the four disulfide bonds[10]. As lysozyme is less prone to unfold, it is considered a hard protein. Lysozyme typically maintains its antibacterial properties after adsorption on inorganic material[11] or in the form of amyloid structures obtained after heating at pH 2 for several hours [12]. For this reason, lysozyme is employed for many applications, from medicine to food industry[13]. More recently, lysozyme has been used to solubilize nanoparticles, such as gold[14] and copper[15], opening new avenues for the development of affordable alternatives to gold for sensing[16,17].

Lysozyme is often used as a model for basic studies of PE-protein complexes[2]. Such complexes can adopt many different structures (gel, microgel micelle, colloid, precipitate, coacervate) by tuning the lysozyme/PE ratio as well as the PE nature and length[2,18–20]. When mixed with polystyrene

sulfonate (PSS) at a [-]/[+] ratio of about 1 ([-] and [+] refer to the concentration of PE and lysozyme, respectively, at neutral pH), such complexes adopt a colloid structure, while lysozyme maintains its antibacterial activity. However, these complexes become unstable in the presence of increasing salt concentrations. With the increase of the [-]/[+] ratio in PSS, lysozyme unfolds and loses its activity[2]. To improve the stability of PE-protein complexes in the presence of salts, methoxypoly(ethylene glycol) -*block*-poly(l-aspartic acid sodium salt) has been used to form micelle structures[20]. However, encapsulation in the micelle structure modifies the lysozyme α-helix/β-sheet ratio [20]. Consequently, the structure dependence of lysozyme when associated with PE has only been investigated through large structural modifications or antibacterial activity. On the other hand, we recently reported that amyloid fibrillation and/or adsorption of lysozyme on layered material modifies its global structure, whereas the integrity of the active site is less affected[11,12]. Several questions remain unanswered, especially about the correlation between enzymatic activity and the integrity and accessibility of the active site in PE-lysozyme (PE-LYS) complexes.

To address these issues, we studied PE-LYS colloids because these complexes are suitable for several applications in catalysis, drug delivery, and entrapment. We considered four different PEs: poly(sodium 4-styrenesulfonate) (PSS), poly(acrylic acid) (PAA), dextran sulfate (DS), and chondroitin 4-sulfate (CS). First, for each PE, we characterized the PE-LYS complex stability in function of the salt concentration by diffusion light scattering. Then, we evaluated the integrity and accessibility of the enzymatic site by fluorescence quenching and time resolved fluorescence analysis. Finally, we analyzed the antibacterial activity of the different PE-LYS complexes.

## 2. Materiel and methods

### *2.1. Material*

Lysozyme (M=14300 g $mol^{-1}$, 6297), PSS ($M_w$~70000 $g.mol^{-1}$, 243051), PAA ($M_w$~100000 $g.mol^{-1}$, 523925), CS sodium salt from bovine trachea (27042), DS sodium salt from *Leuconostoc spp* ($M_w$~6500-10000 g $mol^{-1}$, D 4911), NaCl (S7653), acrylamide (01700), and hydrazine (225819) were purchased from Sigma-Aldrich. $CuSO_4$ (22-36/38) was purchased from Prolabo. Non-pathogenic

*Staphylococcus epidermidis* (CIP53.124) was purchased from Pasteur Institute Laboratory, Lyon, France. Lysogeny broth (LB) Miller culture medium (ref. n°1214662) was purchased from Fischer Scientific, France.

### *2.2. Polyelectrolyte-Lysozyme (PE-LYS) colloid complex preparation*

PE-LYS complexes were obtained by adding 50 µl of lysozyme solution (concentration = 10 mg $ml^{-1}$) and 320 µl of PE (PAA, PSS, CS or DS, concentration = 0.5 mg $ml^{-1}$) to 14.63 ml of deionized water. The resulting colloids were named PAA-LYS, PSS-LYS, CS-LYS, and DS-LYS.

### *2.3. Antibacterial experiments*

Non-pathogenic *Staphylococcus epidermidis* (CIP53.124, from Pasteur Institute Laboratory, Lyon, France) was chosen as surrogate microorganism of bacterial contamination.

**Preparation of the bacterial suspensions used for antibacterial tests**: For each experiment, a new bacterial suspension was prepared from a frozen *S. epidermidis* aliquot. The frozen inoculum (2 mL) was first transferred in LB medium (10 mL). at 37 °C under constant stirring (110 rpm) for 3h. Then, it was inoculated in fresh LB medium (5% *v/v*) and incubated at 37 °C under constant stirring (110 rpm) overnight until the bacteria reached the stationary growth phase. Afterwards, bacteria were pelleted by centrifugation (3300 *g,* 4°C, 20 min) to remove nutrients, and avoid bacterial development in the reactor. The recovered bacterial pellets were suspended in spring water (Cristaline Sainte Cécile, France: $[Ca^{2+}]$ = 39 mg $L^{-1}$, $[Mg^{2+}]$ = 25 mg $L^{-1}$, $[Na^{+}]$ = 19 mg $L^{-1}$, $[K^{+}]$ = 1.5 mg $L^{-1}$, $[F^{-}]$ < 0.3 mg $L^{-1}$, $[HCO_3^{-}]$ = 290 mg $L^{-1}$, $[SO_4^{2-}]$ = 5 mg $L^{-1}$, $[Cl^{-}]$ = 4 mg $L^{-1}$, $[NO_3^{-}]$ < 2 mg $L^{-1}$). The bacterial concentration in the suspensions was determined from the absorbance at 600 nm by using a previously obtained calibration curve. Bacterial cells were finally diluted in spring water to obtain a bacterial suspension in which the cell concentration was about $10^4$ CFU $mL^{-1}$. Each bacterial suspension was instantly used for the antimicrobial tests.

**Counting viable bacteria.** Bacteria were counted using the conventional method of colony counting on agar plates. Each *S. epidermidis* sample was diluted by a factor of 10 in spring water. Each dilution

was spread on LB nutrient agar plates, and plates were incubated at 37°C for 24h to allow bacterial colonies to form. Knowing that each colony stemmed from one initial bacterium, the bacterial concentration in each sample was calculated as the mean number of counted colonies divided by the inoculated volume on LB agar plates, by taking into account the corresponding dilution factor. The quantification limit was 10 CFU $mL^{-1}$. Each counting was done in duplicate and independently.

**Assessment of the antibacterial properties of free lysozyme, and PE-LYS colloids:** Bactericidal tests were carried out in a batch mode, in glass Erlenmeyer flasks (25 mL). Reactions were performed in sterile conditions, at 37° C, and under constant stirring (110 rpm) on a rotary shaker. For each test, 9 mL of bacterial suspension was mixed with 1 mL of lysozyme solution or PE-LYS colloid suspensions (prepared in deionized water). The final lysozyme concentration was 3 µg $L^{-1}$ of lysozyme equivalent. The initial bacterial concentration $C_0$ was precisely determined by the counting method and the mean $C_0$ was 9.8 ± 0.4 x $10^3$ CFU $mL^{-1}$. At the end of the test (3h of incubation at 37° C), the concentration of viable bacteria was measured again using the counting method. Changes in the bacterial concentration were correlated with the bactericidal performances of the tested material. The bacterial concentration decrease was expressed in log-removal values; the log-removal was defined as the logarithm (base 10) ratio of the bacterial concentration C (CFU $mL^{-1}$) measured at 3h to the initial bacterial concentration $C_0$ (CFU $mL^{-1}$). In the case of total removal, a log-removal value of -log ($C_0$) (i.e., – 4.0) was attributed.

### *2.4. Physical characterization*

The UV absorbance spectra were recorded on a JASCO V-570 UV–Vis spectrophotometer at 1 nm $s^{-1}$ scanning rate.

The diffusion coefficients of PE-LYS colloidal complexes were measured by diffusion light spectroscopy (DLS) (Nanophox, Sympatec, France) at 25°C. From the raw data, the diffusion coefficients were obtained using the Quickfit software[21]. A Levenberg-Marquardt non-linear fit without constraint box was used. Two criteria were considered for the fit quality: 1) the $R^2$, and 2) the symmetrical distribution of the residual function. The hydrodynamic radius ($r_H$) of the colloids was

deduced from the diffusion coefficient ($D$) using the Stoke-Einstein equation (equation 1) and assuming a spherical shape:

$$D = \frac{k_B T}{6\pi\eta r} \quad (1)$$

where $k_B$, $T$ and $\eta$, are the Boltzmann constant, the temperature, and the viscosity, respectively.

Time-resolved and steady state fluorescence data were obtained using the time-correlated single-photon counting technique with a previously described home-made set-up[22,23]. Briefly, the excitation wavelength was achieved using a SuperK EXTREME laser (NKT Photonics, model EXR-15) as a continuum pulsed source combined with SuperK EXTEND-UV supercontinuum (NKT Photonics, model DUV). The repetition rate was set to 38.9 MHz; the excitation pulse duration on this device is around 6 ps (full-width-at-half-maximum, FWHM). The fluorescence emission is detected after passing through a polarizer oriented at the magic angle (54.73°) to the polarization of the excitation, through a double monochromator Jobin–Yvon DH10 on a hybrid PMT detector HPM-100-40 (Becker & Hickl). The pulse response function of the equipment was measured by using a diluted suspension of polystyrene nanospheres in water (70 nm of diameter) as scattering solution; FWHM was about 130-160 ps. Decays were collected at a maximum counting rate of 15 kHz in 4096 channels using a SPC-730 acquisition card (Becker & Hickl). All decays were collected with at least 1.5 $10^6$ counts in total. Decay analysis was performed using a Levenberg–Marquardt algorithm. For the analysis, the fluorescence decay law at the magic angle $I_M(t)$ was assumed as the sum of exponentials. Fluorescence lifetime values were calculated from data collected at the magic angle by iterative adjustment after convolution of a pump profile (scattered light) with a sum of exponentials. All details about the calculation of fluorescence lifetime values are given elsewhere[23].

## 3. Results and discussion

### *3.1. Impact of salinity on PE-LYS colloid stability*

PE-LYS complexes were prepared in water using low protein concentration (33 µg $ml^{-1}$). The used [-]/[+] ratio was about 0.01 for PSS and PAA, and about 0.2 for CS and DS. Indeed, it was shown that at

[-]/[+] ratios <1, PSS-LYS complexes adopt a colloidal structure[2]. Dynamic light scattering was used to investigate the impact of increasing NaCl concentrations on the diffusion coefficient and stability of PE-LYS colloids (Fig. 1). First, at low NaCl concentrations, the PEs could not be detected by DLS, and lysozyme diffusion coefficient was about 128 $\mu m^2 s^{-1}$. For the PE-LYS complexes, the fit of the autocorrelation function required two components that depend on the salt concentration (Fig. 2). In water, the fastest component ($D_1$ = 13.72 $\mu m^2 s^{-1}$, 10.27 $\mu m^2 s^{-1}$, 9.76 $\mu m^2 s^{-1}$, and 14.55 $\mu m^2 s^{-1}$ for PAA-LYS, PSS-LYS, CS-LYS, and DS-LYS, respectively) represented the predominant species in the solution (respectively 99.8%, 99.7%, 99.6% and 99.8% according to the pre-exponential factor and assuming a spherical shape for all PE-LYS complexes). It corresponded to spherical colloids with a hydrodynamic radius of 16 nm, 21 nm, 22 nm, and 15 nm for PAA-LYS, PSS-LYS, CS-LYS, and DS-LYS, respectively. Such PE-LYS colloids have been already described[1,3,24]. The slower component ($D_2$ = 3.80 $\mu m^2 s^{-1}$, 3.02 $\mu m^2 s^{-1}$, 3.48 $\mu m^2 s^{-1}$, 3.90 $\mu m^2 s^{-1}$ for PAA-LYS, PSS-LYS, CS-LYS and DS-LYS, respectively) corresponded to larger objects. These large colloids could be assigned to small colloid aggregates that coexist through a dynamic equilibrium. For all PE-LYS colloids, NaCl addition induced a shift of the correlation function toward longer times until signal loss that occurred when the colloids were totally destroyed. For all PE-LYS colloids, the values of the diffusion coefficients $D_1$ and $D_2$ decreased with the increase of NaCl concentration (Fig. 2). This indicates that the size of the two components of the complexes grew. This observation is not surprising because electrostatic interactions are predominant in the formation of PE-LYS colloids. With the increase of the salt concentration, the PE charges were shielded, inducing two effects. The first one was the swelling of colloids due to the introduction of hydrated ions in the PE-LYS complex. This ultimately led to the colloid dissociation, as indicated experimentally by the loss of the DLS signal. The second effect was the colloid aggregation that was characterized by the decrease of the diffusion coefficient. These two effects co-existed because the aggregation allowed minimizing the colloid global energy, counterbalancing their destabilization due to swelling. Interestingly, the colloid aggregation and stability depended on the PE nature. PAA-LYS complexes were the least affected by NaCl addition, and the colloids were not dissociated in the presence of 300 mM NaCl. On the other hand, PSS-LYS complexes were dissociated in the presence of 200 mM NaCl. Although the electrostatic interactions

180 are the primary factor responsible for colloid formation, weak interactions also can play a role.
181 Typically, PAA carboxylic acid moieties are involved in H-bond formation, whereas PSS is prone to
182 hydrophobic interactions. As lysozyme is a hard protein, it should not be unfolded in the complex.
183 Consequently, its surface should be globally hydrophilic and more prone to H-bond formation than to
184 hydrophobic interactions. H-bonds enter in competition with the screening charge due to the increased
185 salt concentration, thus limiting colloid swelling. In PAA-LYS complexes, the aggregation
186 phenomenon is sufficient to counterbalance the colloid destabilization. Like PAA, DS and CS also can
187 form H-bonds with lysozyme. However, they are less charged than PAA, and this could explain why
188 DS-LYS and CS-LYS colloidal complexes were less stable than PAA-LYS complexes. Moreover,
189 dynamic light scattering experiments showed that upon NaCl addition, DS-LYS colloids were more
190 stable than CS-LYS colloids that were dissociated in the presence of 100 mM NaCl. This result can be
191 explained by the number of anionic moieties on each saccharide unit (2 for DS and 1 for CA).

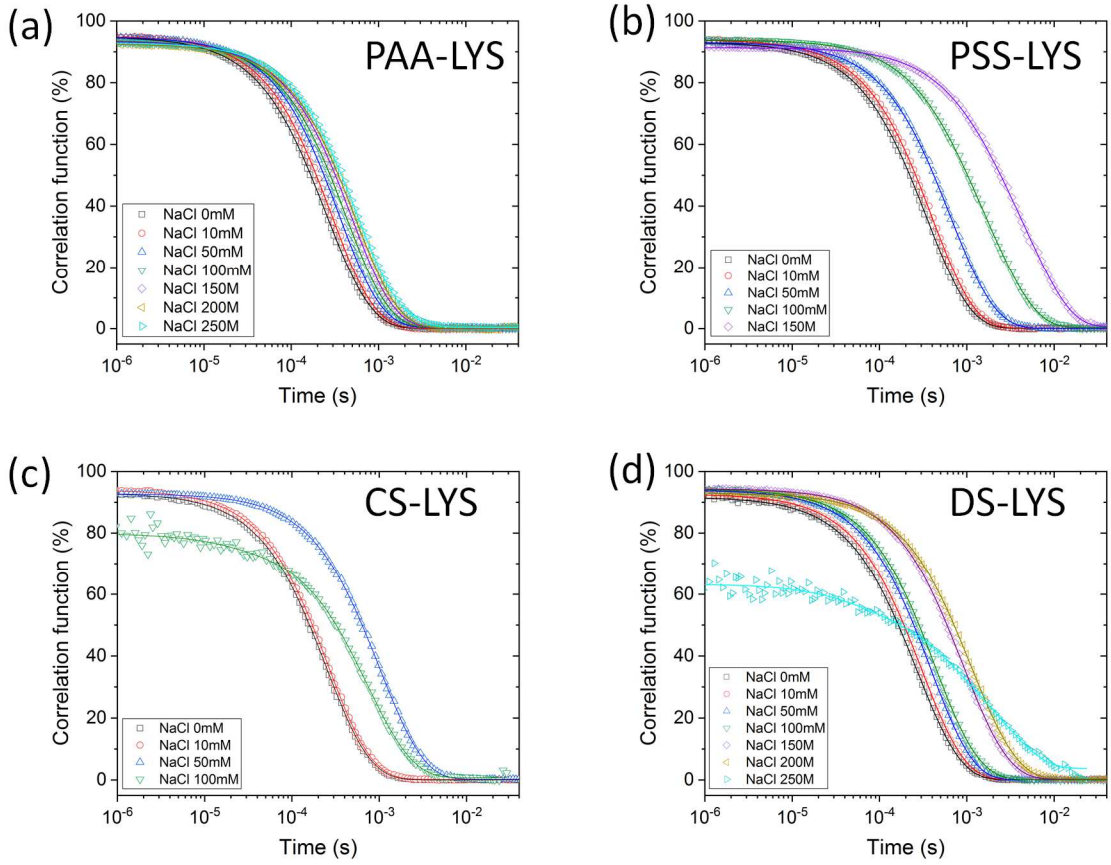


Figure 1: Autocorrelation curves obtained by DLS for (a) PAA-LYS complexes, (b) PSS-LYS complexes, (c) CS-LYS complexes, and (d) DS-LYS complexes at different NaCl concentrations. Symbols and lines represent the experimental measurements and the fits, respectively.

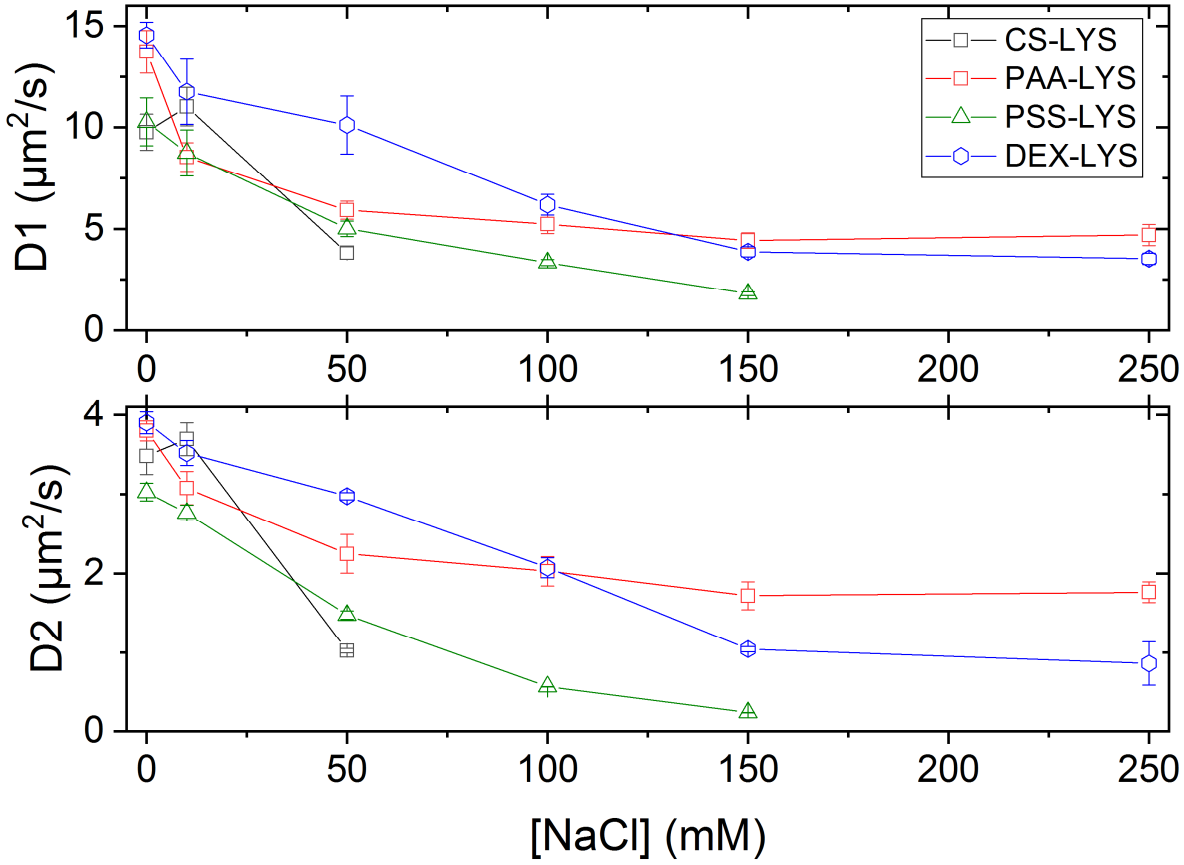


196

197 Figure 2: Diffusion coefficients measured by DSL as a function of NaCl concentration. D1 is the
198 shorter and D2 the longer component. Error bars indicate the standard deviation (n=4). In figure
199 change DEX into DS.

200

201 ***3.2. Accessibility and integrity of lysozyme active site***

202 The active site of lysozyme is located between the α- and β-domains of the protein. It contains three
203 tryptophan residues (Trp62, Trp63, and Trp108) that are important for the enzymatic activity [25].
204 Analysis of its accessibility and integrity showed that at 345 nm, Trp63 fluorescence was quenched by
205 neighboring disulfide bonds, while 92% of the total fluorescence signal was due to the Trp62 and
206 Trp108 residues. Their photophysical properties are strongly affected by the environment inside the
207 active site, and thus by structural modifications [11,12]. Moreover, the fluorescence emission of these
208 Trp residues is quenched when a molecule, such as acrylamide, enters the active site[26]. Therefore,

209 they represent ideal probes to investigate PE impact on the active site accessibility and integrity and
210 for correlations with the antibacterial activity.

211 Quantification of the fluorescence decay of free lysozyme (Fig. 3a) showed that in water, the mean
212 lifetime ($\tau_0$) of lysozyme was 2.34 ns. However, the fluorescence decay fit required four components,
213 in agreement with our previous work [12]. The shorter one ($\tau_4$ = about 0.01 ns with a yield of 2%)
214 could be assigned to the contribution of Trp28 and Trp111, two residues located outside the active site
215 [27]. The three other components ($\tau_1$ = 3.64 ns, $\tau_2$ = 1.62 ns and $\tau_3$ = 0.48 ns with yields of 41 %, 48%
216 and 9%, respectively) were assigned to Trp62 and Trp108.

217 Table 1: Fluorescence lifetime ($\tau_i$), results (mean ± standard deviation) for free lysozyme (LYS) and
218 PE-LYS, obtained with an excitation wavelength of 294 nm and recorded at 345 nm.

| | $\tau_1$ (ns) | $\tau_2$ (ns) | $\tau_3$ (ns) | $\tau_4$ (ns) | $Y_1$ (%) | $Y_2$ (%) | $Y_3$ (%) | $Y_4$ (%) | $\chi^2$ | $\tau_0$ (ns) |
|---|---|---|---|---|---|---|---|---|---|---|
| LYS | 3.64±0.25 | 1.62±0.12 | 0.48±0.05 | 0.01±0.01 | 41 | 48 | 9 | 2 | 1.17 | 2.34±0.26 |
| PAA-LYS | 3.86±0.22 | 1.33±0.11 | 0.40±0.04 | 0.01±0.01 | 33 | 44 | 20 | 4 | 1.12 | 1.93 ±0.25 |
| PSS-LYS | 4.46±0.3 | 1.62±0.13 | 0.45±0.05 | 0.02±0.01 | 36 | 45 | 17 | 2 | 1.11 | 2.39±0.28 |
| CS-LYS | 4.17±0.26 | 1.58±0.11 | 0.46±0.02 | 0.01±0.01 | 40 | 44 | 14 | 2 | 1.15 | 2.43±0.19 |
| DS-LYS | 4.62±0.30 | 1.70±0.10 | 0.46±0.04 | 0.02±0.01 | 41 | 42 | 15 | 2 | 1.07 | 2.68±0.22 |

219

220 Calculation of the fluorescence decays of lysozyme within PE-LYS complexes also required four
221 components. The value and yield of the shorter component $\tau_4$ were not significantly modified in the
222 PE-LYS complexes compared with free lysozyme, suggesting that no large protein structural
223 modification occurred close to the location of Trp28 and Trp111 inside the protein chain. Conversely,
224 lysozyme complexation with PE affected differently the value and the yield of the other components.
225 Indeed, complexation with PAA and DS modified significantly the mean lifetime ($\tau_0$) compared with

PSS and CS (Table 1). Conversely, $\tau_1$ and $\tau_2$ values and/or their yields were affected by all PEs. This could be explained by two hypotheses: (i) PE penetration inside the active site and interaction with the Trp residues, and/or (ii) modification of the active site structure. These hypotheses were tested using the acrylamide test. Indeed, if the active site is crowded by PE molecules, acrylamide will not quench the Trp fluorescence. Addition of acrylamide induced fluorescence quenching in free lysozyme and also in all PE-LYS colloidal complexes (Fig. 3b). This effect involved both dynamic and static processes that can be expressed by the following equation:

$$\frac{F_0}{F_{\{Q\}}} = (1 + K_{SV}\{Q\})(1 + K_S\{Q\}) \quad (2)$$

where $F_0$ and $F_{\{Q\}}$ are the fluorescence intensity at the quencher concentration =0 and =$\{Q\}$ respectively, $K_{SV}$ is the Stern-Volmer constant (eq. 3) relative to the collisional quenching process[28], and $K_S$ is the constant of the formation of a ground-state non-fluorescent complex. The Stern-Volmer constant can be obtained from the linear dependence of $\frac{\tau_0}{\tau_{\{Q\}}}$ as a function of $\{Q\}$ (Fig. 3c). The $K_{SV}$ Stern-Volmer constant reached 4.65 $M^{-1}$ for free lysozyme and decreased for PE-LYS colloids (Table 2). A lower $K_{SV}$ could be due to a structural modification or a reduced accessibility of the active site due to PE presence. To elucidate the origin of $K_{SV}$ reduction, the quenching rate constant ($k_q$) was calculated from the fluorescence lifetime value ($\tau_0$) (eq. 3):

$$\frac{\tau_0}{\tau_{\{Q\}}} = 1 + K_{SV}\{Q\} \quad = 1 + k_q\tau_0\{Q\} \quad (3)$$

Comparison of the quenching rate constant ($k_q$) values (Table 2) showed that they were decreased when lysozyme was complexed with PE. This could directly be interpreted as a decrease of the acrylamide/Trp collisions. The decrease of dynamic quenching could originate from (i) a modification of the active structure site, and/or (ii) a decrease of the active site accessibility due to PE steric effect. As Trp quenching by acrylamide involved also static processes, the $K_S$ was calculated by plotting the $\frac{I_0}{I}\left(\frac{\tau_0}{\tau_{\{Q\}}}\right)^{-1}$ as a function of acrylamide concentration (Fig. 3d). For free lysozyme in water, a linear dependence was observed with $K_S$= 2.04 $M^{-1}$. This linear dependence was maintained only when

lysozyme was complexed with PSS, but with a lower $K_S$ value (1.22 $M^{-1}$). This means that the active site is more accessible in PSS-LYS complexes compared with the PE-LYS made with PAA, CS and DS.

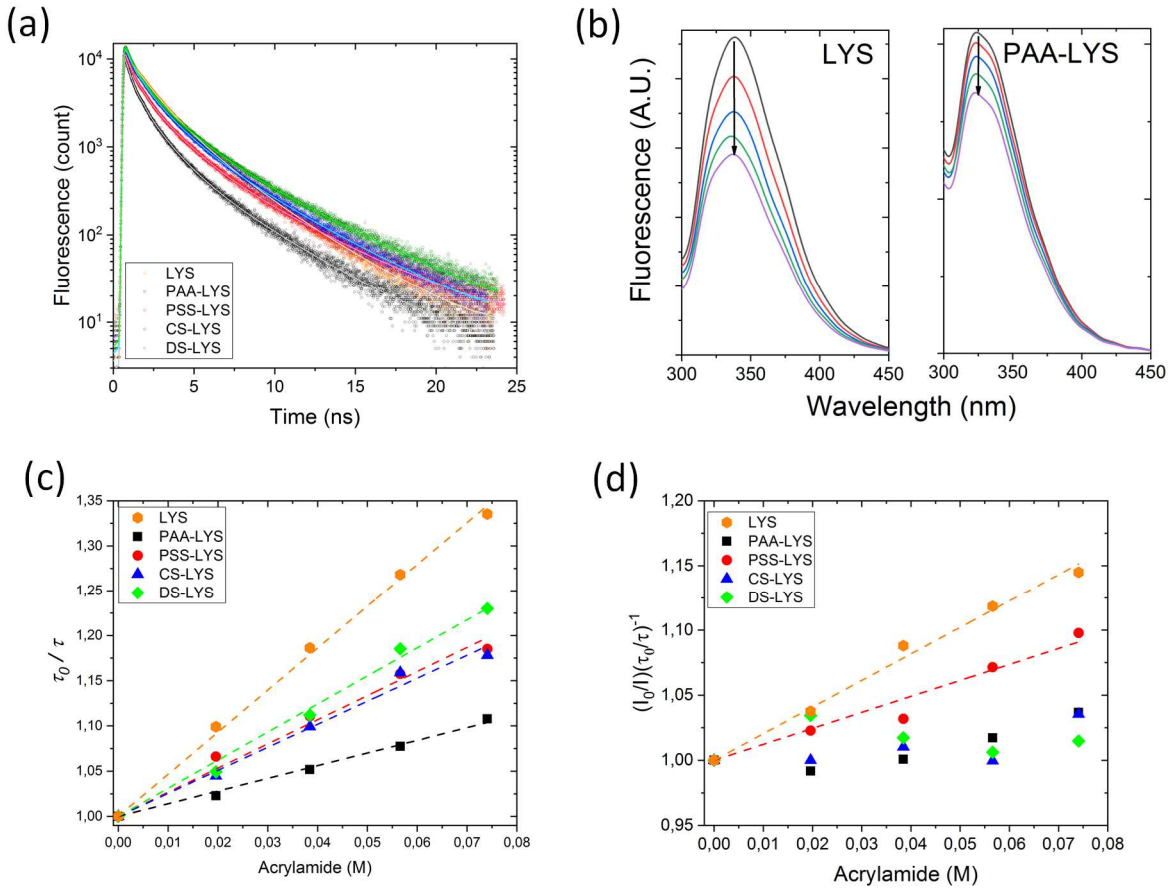


Figure 3: (a) Fluorescence decay (symbol) and fit (line) of free lysozyme (LYS) (orange), PAA-LYS (black), PSS-LYS (red), CS-LYS (blue) and DS-LYS (green) colloidal complexes. (b) Fluorescence emission spectra of LYS and PAA-LYS as a function of the acrylamide concentration: 0 mM (black line), 19 mM (red line), 38 mM (blue line), 56 mM (green line), and 74 mM (violet line). (c) Stern-Volmer plot (symbol) and linear fit (dash line) for LYS and PE-LYS complexes. (d) Plot of $\frac{I_0}{I}\left(\frac{\tau_0}{\tau_{(Q)}}\right)^{-1}$ as a function of acrylamide concentration (symbol), and linear fit (dash line).

Table 2: Values of the Stern-Volmer $K_{SV}$ constant, quenching constant $k_{q,}$ and static quenching constant $K_s$.

| | $K_{SV}\,[M]^{-1}$ | $k_q\,(10^9)[M \times s]^{-1}$ | $Ks\,[M]^{-1}$ |
|---|---|---|---|
| **LYS** | 4.65 | 2.03 | 2.04 |
| **PAA-LYS** | 1.40 | 0.72 | *N.A.* |
| **PSS-LYS** | 2.67 | 1.12 | 1.22 |
| **DS- LYS** | 3.11 | 1.16 | *N.A.* |
| **CS-LYS** | 2.55 | 1.05 | *N.A.* |

In conclusion, our results show that PEs modified the physical properties of the Trp62 and Trp108 residues, and that the active site accessibility was reduced in PE-LYS complexes. The first information is that the active site was not fully crowded by the PE because acrylamide could still quench Trp fluorescence. This means that the fluorescence lifetime changes can be assigned to a structural modification of the active site. This is quite consistent with the fluorescence lifetime results. Indeed, if PE molecules were present inside the active site, their interaction with the Trp residues should have modified the fluorescence lifetime values, especially PSS due to the presence of aromatic moieties. However, our findings indicate that the fluorescence lifetime values were not strongly affected by the PE, although the photophysical property changes were significant. In addition, it is unlikely that PE molecules can enter in the active site due to steric hindrance. Thus, the most probable explanation of the fluorescence lifetime value changes is a structural modification of the active site. Indeed, the active site is located between the β- and the α-domains of the protein. It is constituted by amino acids involved in these domains and in the loop that connects them, thus making it prone to local structural modifications that do not affect the global protein integrity. In some cases, structural modifications of lysozyme especially in the α-domain do not strongly affect the active site, as previously shown for the

281 lysozyme amyloid structure[12]. This result is consistent with previous reports in which structural
282 modification of lysozyme confined in a PE matrix was highlighted by circular dichroism[20]. The
283 second information is that PEs also play a role in the active site accessibility. Indeed, the acrylamide
284 test results showed that lysozyme active site in PE-LYS complexes formed with PSS is more
285 accessible compared with complexes formed with PAA, CS and DS. This is consistent with the high
286 stability of PAA-LYS colloids upon salt addition (Fig. 1a). Indeed, the interactions (electrostatic and
287 H-bonds) between PAA and LYS are stronger, making the colloid structure more compact.
288 Consequently, acrylamide cannot easily diffuse inside these colloids to form the non-fluorescence
289 complex. Conversely, PSS-LYS colloids swell with the increase of salt concentration, because they are
290 less compact. Therefore, acrylamide can easily diffuse inside the structure. Overall, our results clearly
291 demonstrate that colloids based on CS and DS follow the same trend: the combination of electrostatic
292 interactions and H-bond formation makes these colloids less prone to the formation of acrylamide/Trp
293 complexes.

294 ***3.3. Antibacterial activity of PE-LYS colloids***

295 To assess the antibacterial activity of the PE-LYS colloidal complexes against the Gram-positive *S.*
296 *epidermidis*, experiments were performed with the same lysozyme (free or in the colloids)
297 concentration (*i.e.,* 3 µg $L^{-1}$ of lysozyme equivalent). The blank experiment (i.e., bacterial suspension
298 without free lysozyme and PE-LYS) showed that the bacterial concentration remained nearly constant
299 at the end of the 3h incubation (Table 3). As expected, free lysozyme had a strong anti-microbial
300 activity, as indicated by the 2 log-removal value (per absolute value). The PE-LYS colloids exhibited
301 about 1 log-removal values (i.e., 90% of bacteria were killed).. Therefore, our results confirm that
302 lysozyme complexed with PE retains some catalytic activity, and are in agreement with what
303 previously reported for PSS-LYS [2]. It is interesting to note that the PE nature did not influence the
304 log-removal value, indicating that the change in antibacterial activity was not due to a structural
305 modification of the active site, but rather to a decrease of the number of accessible sites, in line with
306 the fluorescence results (section 3.2).

307 Table 3: Bacterial log-removal values (mean ± standard deviation n=3) obtained after incubation of
308 Gram positive *S. epidermidis* with free lysozyme (LYS) and PE-LYS colloidal complexes for 3 hours.

| | Concentration (CFU $mL^{-1}$) | Log-removal values (-) |
|---|---|---|
| Initial bacterial suspension | $9.8 \pm 0.4 \times 10^3$ | |
| Blank (no LYS and PE-LYS) at 3h | $8.5 \pm 0.4 \times 10^3$ | - 0.1 |
| LYS at 3h | $4.0 \pm 0.4 \times 10^1$ | - 2.4 |
| PAA-LYS at 3h | $1.1 \pm 0.1 \times 10^3$ | - 0.9 |
| PSS-LYS at 3h | $1.2 \pm 0.2 \times 10^3$ | - 0.9 |
| DS-LYS at 3h | $9.6 \pm 0.3 \times 10^2$ | - 1.0 |
| CS-LYS at 3h | $1.2 \pm 0.1 \times 10^3$ | - 0.9 |

309

310

311 **4. Conclusion**

312 We investigated the properties of lysozyme involved in colloids with different polyanions. Our results
313 highlight that the PE nature strongly influences the size and stability of PE-LYS colloidal complexes
314 as well as the antibacterial properties of lysozyme when complexed with PEs. Colloids made with
315 PAA, where both electrostatic interactions and H-bond formation are involved, were more compact
316 and more stable than those obtained with PSS. However, the enzyme active sites were less accessible
317 to acrylamide. The complexes formed with polysaccharides (DS and CS) also involved electrostatic
318 interactions and H-bond formation. This led to a compact complex structure that did not allow the
319 formation of Trp-acrylamide complexes. However, due to their lower charge density, compared with
320 DS (and PAA), CS are less stable upon salt addition. On the basis of the fluorescence results, the
321 decreased antibacterial activity observed when lysozyme was complexed with PEs can be explained by
322 the reduced accessibility and a structural modification of the enzyme active site. Our results highlight
323 the role of the PE-LYS structure as a key factor for understanding lysozyme activity.

324

325 **Acknowledgements**

The authors would like to acknowledge the “Institut Européen des Membranes (IEM)-UMR 5635” for supporting this study through the health project PS1-2017.

## References

[1] C.L. Cooper, P.L. Dubin, A.B. Kayitmazer, S. Turksen, Polyelectrolyte-protein complexes, Curr. Opin. Colloid Interface Sci. 10 (2005) 52–78. doi:10.1016/j.cocis.2005.05.007.

[2] F. Cousin, J. Gummel, S. Combet, F. Boué, The model Lysozyme-PSSNa system for electrostatic complexation: Similarities and differences with complex coacervation, Adv. Colloid Interface Sci. 167 (2011) 71–84. doi:10.1016/j.cis.2011.05.007.

[3] J.M. Park, B.B. Muhoberac, P.L. Dubin, J. Xia, Effects of Protein Charge Heterogeneity in Protein-Polyelectrolyte Complexation, Macromolecules. 25 (1992) 290–295. doi:10.1021/ma00027a047.

[4] J. Gummel, F. Cousin, F. Boué, Counterions release from electrostatic complexes of polyelectrolytes and proteins of opposite charge: A direct measurement, J. Am. Chem. Soc. 129 (2007) 5806–5807. doi:10.1021/ja070414t.

[5] B. Krajewska, Application of chitin- and chitosan-based materials for enzyme immobilizations: A review, Enzyme Microb. Technol. 35 (2004) 126–139. doi:10.1016/j.enzmictec.2003.12.013.

[6] F. Caruso, C. Schüler, Enzyme multilayers on colloid particles: Assembly, stability, and enzymatic activity, Langmuir. 16 (2000) 9595–9603. doi:10.1021/la000942h.

[7] L.E. Bromberg, E.S. Ron, Temperature-responsive gels and thermogelling polymer matrixes for protein and peptide delivery, Adv. Drug Deliv. Rev. 31 (1998) 197–221.

[8] N.A. Peppas, W. Leobandung, Stimuli-sensitive hydrogels: Ideal carriers for chronobiology and chronotherapy, J. Biomater. Sci. Polym. Ed. 15 (2004) 125–144. doi:10.1163/156856204322793539.

[9] T. Arai, W. Norde, The behavior of some model proteins at solid-liquid interfaces 1.

Adsorption from single protein solutions, Colloids and Surfaces. 51 (1990) 1–15. doi:10.1016/0166-6622(90)80127-P.

[10] J. Koo, M. Erlkamp, S. Grobelny, R. Steitz, C. Czeslik, Pressure-induced protein adsorption at aqueous-solid interfaces, Langmuir. 29 (2013) 8025–8030. doi:10.1021/la401296f.

[11] S. Balme, R. Guégan, J.-M. Janot, M. Jaber, M. Lepoitevin, P. Dejardin, X. Bourrat, M. Motelica-Heino, Structure, orientation and stability of lysozyme confined in layered materials, Soft Matter. 9 (2013). doi:10.1039/c3sm27880h.

[12] Z. Bouaziz, L. Soussan, J.-M. Janot, M. Lepoitevin, M. Bechelany, M.A. Djebbi, A.B.H. Amara, S. Balme, Structure and antibacterial activity relationships of native and amyloid fibril lysozyme loaded on layered double hydroxide, Colloids Surfaces B Biointerfaces. 157 (2017). doi:10.1016/j.colsurfb.2017.05.050.

[13] T. Wu, Q. Jiang, D. Wuc, Y. Hu, S. Chen, T. Ding, X. Ye, D. Liu, J. Chen, What is new in lysozyme research and its application in food industry? -A review, Food Chem. (2018). doi:10.1016/j.foodchem.2018.09.017.

[14] H. Wei, Z. Wang, J. Zhang, S. House, Y.G. Gao, L. Yang, H. Robinson, L.H. Tan, H. Xing, C. Hou, I.M. Robertson, J.M. Zuo, Y. Lu, Time-dependent, protein-directed growth of gold nanoparticles within a single crystal of lysozyme, Nat. Nanotechnol. 6 (2011) 93–97. doi:10.1038/nnano.2010.280.

[15] R. Ghosh, A.K. Sahoo, S.S. Ghosh, A. Paul, A. Chattopadhyay, Blue-emitting copper nanoclusters synthesized in the presence of lysozyme as candidates for cell labeling, ACS Appl. Mater. Interfaces. 6 (2014) 3822–3828. doi:10.1021/am500040t.

[16] X. Hu, T. Liu, Y. Zhuang, W. Wang, Y. Li, W. Fan, Y. Huang, Recent advances in the analytical applications of copper nanoclusters, TrAC - Trends Anal. Chem. 77 (2016) 66–75. doi:10.1016/j.trac.2015.12.013.

[17] Y. Guo, F. Cao, X. Lei, L. Mang, S. Cheng, J. Song, Fluorescent copper nanoparticles: Recent

advances in synthesis and applications for sensing metal ions, Nanoscale. 8 (2016) 4852–4863. doi:10.1039/c6nr00145a.

[18] C. Johansson, P. Hansson, M. Malmsten, Interaction between lysozyme and poly(acrylic acid) microgels, J. Colloid Interface Sci. 316 (2007) 350–359. doi:10.1016/j.jcis.2007.07.052.

[19] C. Johansson, J. Gernandt, M. Bradley, B. Vincent, P. Hansson, Interaction between lysozyme and colloidal poly(NIPAM-co-acrylic acid) microgels, J. Colloid Interface Sci. 347 (2010) 241–251. doi:10.1016/j.jcis.2010.03.072.

[20] F.G. Wu, Y.W. Jiang, Z. Chen, Z.W. Yu, Folding Behaviors of Protein (Lysozyme) Confined in Polyelectrolyte Complex Micelle, Langmuir. 32 (2016) 3655–3664. doi:10.1021/acs.langmuir.6b00235.

[21] J. Krieger, J. Langowski, QuickFit 3.0 : A data evaluation application for biophysics, (2015). http://www.dkfz.de/Macromol/quickfit/.

[22] V. Tangaraj, J.-M. Janot, M. Jaber, M. Bechelany, S. Balme, Adsorption and photophysical properties of fluorescent dyes over montmorillonite and saponite modified by surfactant, Chemosphere. 184 (2017). doi:10.1016/j.chemosphere.2017.06.126.

[23] S. Balme, J.-M. Janot, P. Déjardin, P. Seta, Highly efficient fluorescent label unquenched by protein interaction to probe the avidin rotational motion, J. Photochem. Photobiol. A Chem. 184 (2006). doi:10.1016/j.jphotochem.2006.04.016.

[24] F. Cousin, J. Gummel, D. Ung, F. Boué, Polyelectrolyte-protein complexes: Structure and conformation of each specie revealed by SANS, Langmuir. 21 (2005) 9675–9688. doi:10.1021/la0510174.

[25] E. Nishimoto, S. Yamashita, A.G. Szabo, T. Imoto, Internal motion of lysozyme studied by time-resolved fluorescence depolarization of tryptophan residues, Biochemistry. 37 (1998) 5599–5607. doi:10.1021/bi9718651.

399 [26] Y. Tokunaga, Y. Sakakibara, Y. Kamada, K.I. Watanabe, Y. Sugimoto, Analysis of core region
400 from egg white lysozyme forming amyloid fibrils, Int. J. Biol. Sci. 9 (2013) 219.
401 doi:10.7150/ijbs.5380.

402 [27] S. Yamashita, E. Nishimoto, N. Yamasaki, The Steady State and Time-resolved Fluorescence
403 Studies on the Lysozyme-Ligand Interaction, Biosci. Biotechnol. Biochem. 59 (2009) 1255–
404 1261. doi:10.1271/bbb.59.1255.

405 [28] A.M. Edwards M., E. Silva S., Exposure of tryptophanyl residues in ??-lactalbumin and
406 lysozyme - Quantitative determination by fluorescence quenching studies, Radiat. Environ.
407 Biophys. 25 (1986) 113–122. doi:10.1007/BF01211735.

408 [

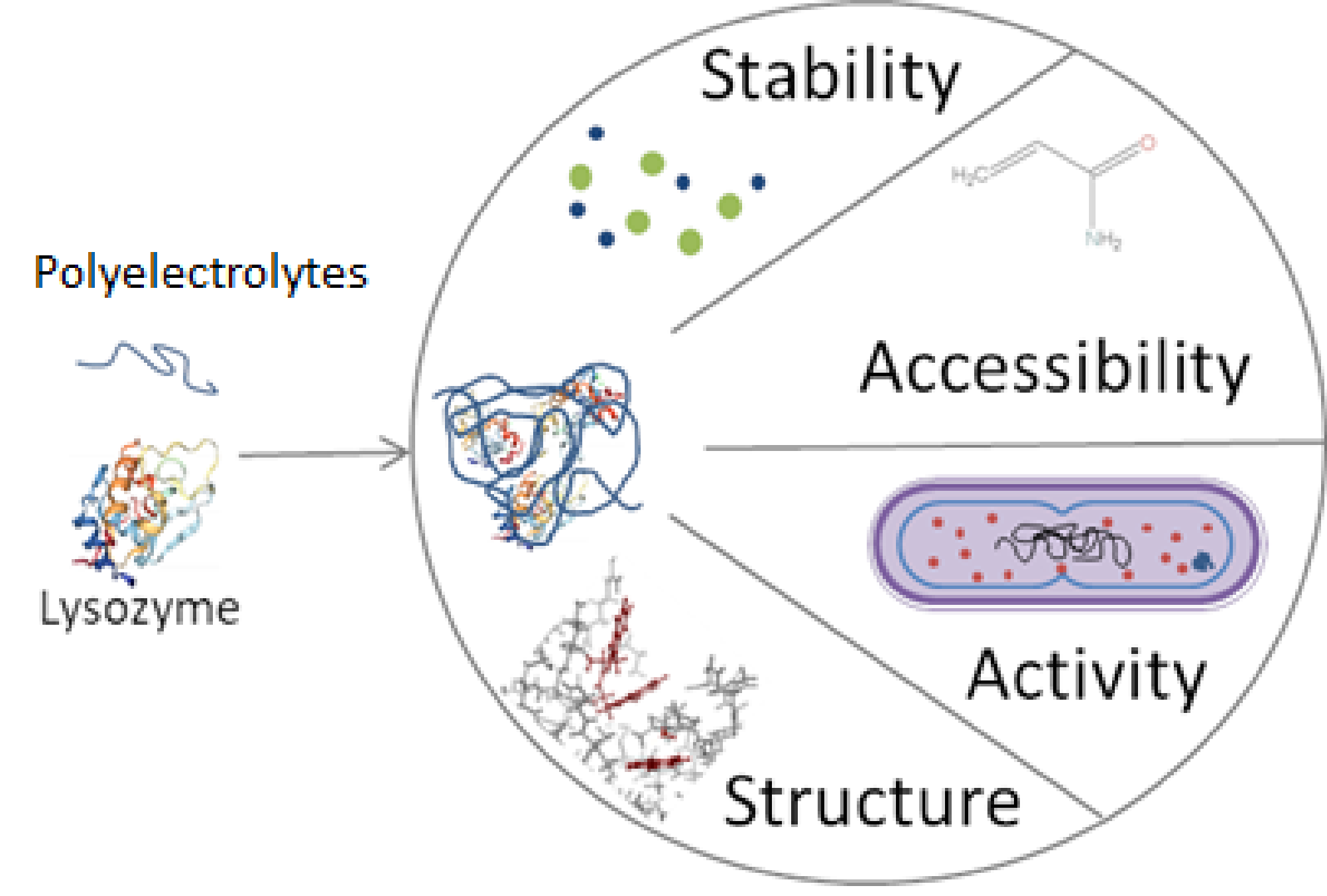
Polyelectrolytes
Lysozyme
Stability
Accessibility
Activity
Structure